Journal of Applied Polymer Science

Dynamics of migration and phase selective localization of nanoclay in HNBR/ENR blends

Zulfiqar Ali,[1] Hai Hong Le,[2] Javed Iqbal,[1] Murid Hussain,[1] Hazrat Hussain,[3] Nasir Mahmood,[4] Ahmad Nawaz Khan,[5] HansJoachim Radusch[2]

[1]Department of Chemical Engineering, COMSATS Institute of Information Technology, 54000 Lahore, Pakistan
[2]Department of Polymer Technology, Center for Engineering Sciences, Martin Luther University Halle-Wittenberg, D-06099 Halle (Saale), Germany
[3]Department of Chemistry, Quaid-i-Azam University Islamabad, Islamabad, 45320, Pakistan
[4]Institut Für Chemie, Martin Luther University Halle-Wittenberg, Halle, Saale, D-06099, Germany
[5]School of Chemical & Materials Engineering, National University of Sciences and Technology (NUST) H12, Islamabad
Correspondence to: H. Hussain (E-mail: hazrat.hussain@qau.edu.pk) and Z. Ali (E-mail: zulfiqar.ali@ciitlahore.edu.pk)

ABSTRACT: The phase specific selective localization and dynamics of migration of nanoclay in hydrogenated acrylonitrile butadiene rubber (HNBR)/epoxidized natural rubber (ENR) blend systems is investigated. The phase specific dispersion of clay particles is monitored through measuring the online measured electrical conductance (OMEC) during mixing by means of a sensor system installed inside the chamber of an internal mixer. The results of different characterization techniques, such as atomic force microscopy, transmission electron microscopy, and small angle X-ray scattering have been used to understand and interpret the OMEC behaviors of nanoclay-filled rubber compounds individually (HNBR and ENR) and their blend systems. The observed online conductance is ionic in nature that arises due to the release of surfactant molecules from the clay galleries. It is observed that the OMEC behavior depends mainly on two factors: the localization of nanoclay in specific phase of the blend system and on the gradual development of blend morphology. The OMEC behavior and the supported data from the microscopic methods, clearly reveal the migration of organoclay from the ENR to HNBR phase during the mixing process, particularly localizing near the interface of the blend. Further, the localization of organoclay is also evaluated by applying the surface tension measurements based model, which also predicts the favorable localization of organoclay in HNBR phase of the blend. The work clearly suggests the OMEC method to be a powerful online tool to monitor and control the nanoclay dispersion and localization in rubber based nanocomposites during the melt mixing process.
 J. Appl. Polym. Sci. **2016**, *133*, 44074.

KEYWORDS: blends; clay; composites

Received 22 February 2016; accepted 15 June 2016
DOI: 10.1002/app.44074

INTRODUCTION

Exorbitant market demands for new polymeric materials that can be met either by synthesizing new materials or blending and filling the existing ones. The latter one is easy to process and finds commercial applications. Recently, the incorporation of nanoclay into rubber blends is finding increasing interest in industrial and scientific research.[1–5] In literature, a large number of works have been reported regarding the enhancement of tribological and mechanical properties,[6–8] chemical and thermal stability.[9–11] For nanocomposites, based on rubber blends, it has been extensively reported that clay prefers to stay in the blend phase which has better affinity for nanoclay. However, if the affinity of both phases of the blend for clay is the same, then it preferentially resides at the interphase.[12–18] Organoclay at the interface causes an effective size reduction of the dispersed phase, narrowed size distribution,[19,20] and enhanced compatibility in the blend by reducing the surface energy gap between the blend components.[21–23] Generally, the distribution and dispersion of nanoclay in polymer blends and the development of the blend morphology is characterized by post processing techniques, for instance, transmission electron microscopy (TEM), atomic force microscopy (AFM), and scanning electron microscopy (SEM). Owing to increasing demands with respect to productivity, quality, and commercialization of the products, it is highly desirable to have an online technique that provides real time information about morphological changes at different stages of mixing process. In previous studies by some of the authors of this paper,[24,25] the method of online measured

electrical conductance (OMEC) was introduced for controlling the mixing of carbon black in nonpolar/nonpolar ethylene-propylene diene terpolymer/styrene-butadiene rubber (EPDM/SBR) blends and nanoclay in polar/nonpolar HNBR/NR blends. The present work focuses with the phase specific nanoclay localization and the development of blend morphology in polar/polar hydrogenated acrylonitrile butadiene rubber (HNBR)/epoxidized natural rubber (ENR) blend systems by employing OMEC, TEM, AFM, small angle X-ray scattering, surface tension measurement, and stress-strain analysis techniques.

EXPERIMENTAL

Materials

Commercially available hydrogenated acrylonitrile butadiene rubber (HNBR) with acrylonitrile content of 36 wt % (Zetpol 2030L) was obtained from Zeon Europe GmbH, Germany and epoxidized natural rubber (ENR) with epoxidation grade of 50 wt % was purchased from Weber & Schaer GmbH & Co. KG, Germany and were used as rubber matrix. The epoxy groups were statistically distributed along the main chain of ENR.[26] Organoclay (Nanofil 9), obtained from Süd-Chemie Germany, was used as filler. It was modified by stearyl benzyl dimethyl ammonium chloride surfactant. Our investigations as well as the data of the clay provider show that before compounding, the organoclay has a basal spacing of 2.0 nm. Vulcanization of the rubber compounds was carried out by the Peroxide Luperox 101 (Atofina Chemicals, USA).

Sample Preparation

For sample preparation, an internal mixer, PolyLab System Rheocord (Thermo Electron/Haake, Karlsruhe, Germany) fitted with online electrical conductance measuring sensor was used. The clay dispersion in virgin rubber compounds, HNBR and ENR was characterized by mixing 1.8 wt % peroxide in an internal mixer PolyLab System Rheocord at a rotor speed of 70 rpm and an initial chamber temperature of 50 °C. After complete mastication and mixing of peroxide in rubber compound (7 min), the clay was added to the rubber after 7 min. The clay content of 4.7 wt % was kept constant for all the nanocomposite samples. For preparation of HNBR/ENR/clay blends an ENR/clay masterbatch containing 9.1 wt % of clay was mixed with pure HNBR. In all these blends the ratio of HNBR/ENR was kept constant at 50/50 wt % with overall 4.7 wt % clay content. The dynamics of organoclay dispersion and development of the blend morphology was characterized by taking out the samples from the mixing chamber at different mixing times. The mixing time is the time taken after mixing unfilled HNBR and ENR-clay masterbatch.

After preparing the samples in internal mixer, they were compression molded in compression molding machine, Platten Press (Dr. Collin, Ebersberg, Germany) at 170 °C for time till samples are 90% vulcanized as calculated with the help of Elastograph Vario (Göttfert, Buchen, Germany). Afterward, the temperature was decreased to room temperature to obtain the 120 × 120 mm^2 plates of 1 mm thickness. These compression molded plates were used for the further analysis.

TESTING METHODS

Online Measurement of Electrical Conductance

The electrical conductance signals, during the mixing process, were measured by the conductivity sensor that was installed in the mixing chamber of the internal mixer. The conductance signal also showed good reproducibility.

Atomic Force Microscopy

Atomic force microscope, Q-Scope 250 (Quesant, Santa Cruz, CA), was used to carry out the morphological investigation. It was operated in intermittent mode and equipped with a 40 x 40 μm. The cantilever stiffness is 40 N/m and the resonance frequency nearly 170 kHz. Samples were cryo-cut by means of a microtome HM 360/CM 30 (Microm, Walldorf, Germany) at −100 °C by a diamond knife in order to get a smooth surface.[25]

Transmission Electron Microscopy

Transmission electron microscope, JEM 2010 (Jeol, Peabody, MA), with an operating current of 200 kV was used to analyze the bulk morphology of the samples. The TEM samples (ultrathin sections of 100 nm thickness) were microtomed with ultracut microtome (Leica Microscopy GmbH, Wetzlar Germany) in liquid nitrogen atmosphere at −120 °C and were collected directly on the TEM grid.[25]

Small Angle X-ray Scattering

Small angle X-ray scattering (SAXS) analyses were performed at room temperature using a pinhole instrument designed by JJ X-rays (Kgs. Lyngby, Denmark) with a Rigaku rotating anode as radiation source CuKα tube ($\lambda = 0.154$ nm) for detection of the state of exfoliation by using a generator voltage 40 kV and current 560 mA, respectively. The scattering vector 'q' is defined by $q = 4\pi/\lambda \sin\theta$. The first order Bragg peak in the Lorentz corrected intensity curves were fitted by using a Gaussian function with linear background subtraction, giving the interlayer distance and the relative peak strength. The thickness of all the samples was kept constant, i.e., 1.0 mm, therefore, the amount of ordered structure is reflected by the peak area.

Surface Tension Measurements

Wetting experiments (modified Wilhelmy method) were performed using the dynamic contact angle meter and tensiometer DCAT 21, (DataPhysics Instruments GmbH, Filderstadt, Germany). For Wilhelmy measurements, the clay particles were put in a shallow plate. In the filler powder a 2 × 1 cm^2 piece of a double-face adhesive tape (TESA 55733, Germany), was dipped and gently moved to achieve a uniform coating of the filler platelets on the tape. The pellets of the granulated nanoclay were finely pulverized in a mortar, before they were attached at the adhesive tape. Extra particles that did not stick to the tape, were blown away under nitrogen flow. The clay platelets coated tape without any further modification, was used for Wilhelmy contact angle measurements. Sessile drop contact angle measurements were carried out with an automatic contact angle meter OCA 40 Micro (DataPhysics Instruments GmbH, Germany) on an uncured rubber sheet. The wetting experiment results were used to calculate the surface energies. A set of test liquids, with different polarity and surface tension, formamide (Merck, Germany), dodecane (Merck Schuchardt, Germany), water (Millipore Milli-Q-Quality), ethylenglycol (Fisher Scientifiy,

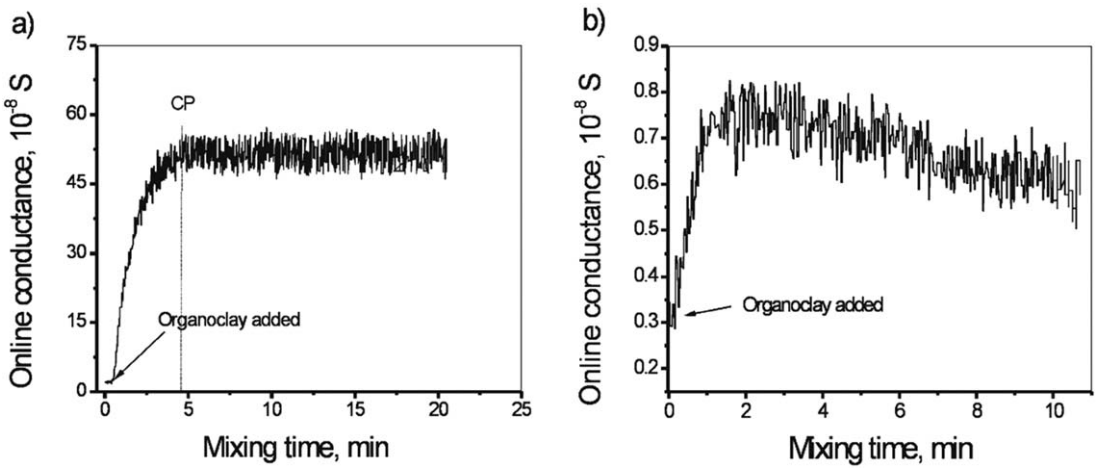

Figure 1. Online measured electrical conductance: (a) HNBR/clay and (b) ENR/clay nanocomposites as function of mixing time.

UK), n-hexadecane (Merck, Germany) and ethanol (Uvasol, Merck, Germany) were used for this purpose. Surface energy analyses were performed by fitting the Fowkes equation.[27]

Tensile Properties

The mechanical properties were evaluated by using stress-strain analyses performed according to ISO 37 using a tensile tester Z005 (Zwick/Roell, Germany), having a cross-head speed of 200 mm/min at room temperature. The samples were vulcanized at 170 °C and compression molded to 1 mm thick sheet. Five dog bone specimens (with thickness of 1 mm and initial length of 50 mm) for each of the sample were analyzed at Universal Testing Machine. The values represented are average of the five analyses.

RESULTS AND DISCUSSION

Dynamics of Clay Dispersion in HNBR And ENR

The online measured electrical conductance curves of HNBR/clay and ENR/clay nanocomposites as function of mixing time are shown in Figure 1. The time represented is the time after addition of organoclay to the rubber matrix. Figure 1(a) shows an initial significant increase in online conductance of HNBR/clay masterbatch with increase in mixing time up to 4 min followed by a plateau. In previous investigations,[28] the increase in online conductance signal after addition of organoclay was attributed to ionic conductance. The movement of quaternary ammonium ions from the nanoclay galleries to the rubber matrix is facilitated by steady motion of the rubber chains during the mixing process. According to Sadhu *et al.*[29] there exists hydrogen bonding between the nitrile group of the rubber and ammonium ions of intercalated surfactants. Thus, it seems that the H-bonding weakens or dissociates, that leads to decrease in the attractive forces between the negatively charged clay surface and the cationic end groups of the alkyl ammonium moiety. As the mixing process proceeds, the contact area between the rubber and organoclay increases due to intercalation and exfoliation of the clay platelets. The net outcome is the release of trapped charged carriers from inside the clay galleries resulting in the higher online conductance.

Figure 1(b) depicts the online conductance of ENR/clay nanocomposite as function of mixing time. The lower level of OMEC of ENR/clay nanocomposite is due to the lower conductivity of ENR compared to HNBR. By comparing Figure 1(a,b), it can be seen that there exists a significant difference in the online conductance behavior of HNBR/clay and ENR/clay

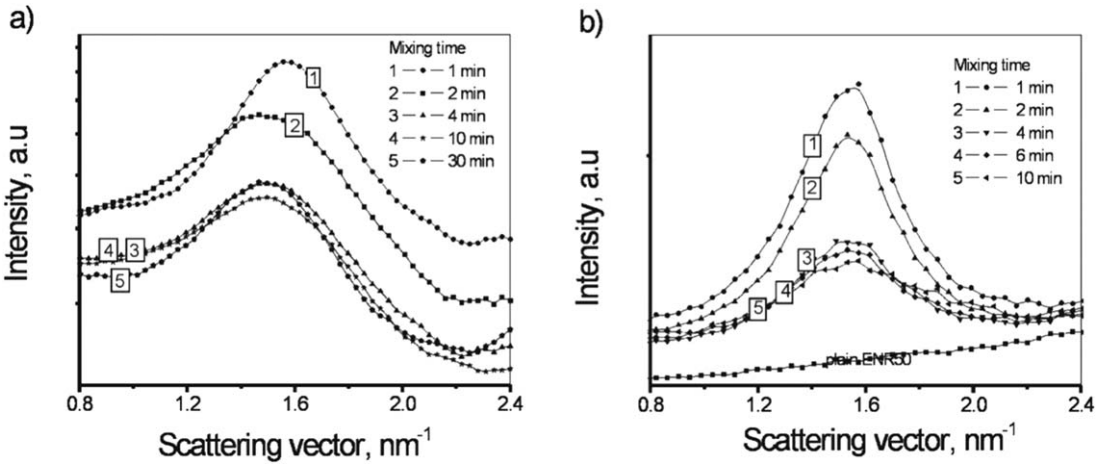

Figure 2. SAXS patterns: (a) HNBR/clay nanocomposite and (b) ENR/clay nanocomposite as function of mixing time.

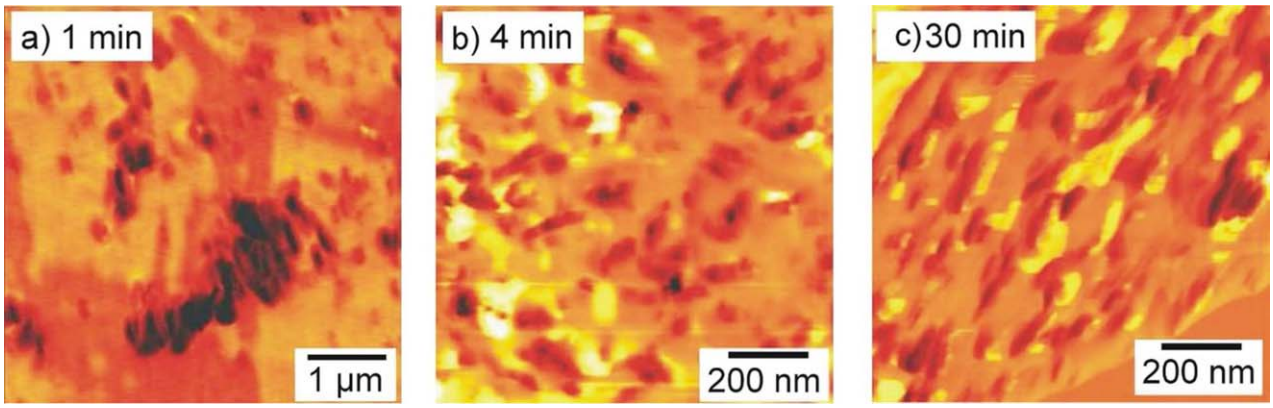

Figure 3. AFM-images of HNBR/clay nanocomposite after various mixing times. [Color figure can be viewed in the online issue, which is available at wileyonlinelibrary.com.]

nanocomposite systems. The conductance of the former passes through a critical point and then remains constant, whereas the conductance of the latter decays after reaching a maximum value.

It can be noted that the increase of OMEC in ENR/clay nanocomposite is due to the release of surfactant molecules, but at the same time the motion of the surfactant molecules is hindered because of the interaction, via *H*-bonding, between the surfactant molecules and epoxy groups of ENR.[30] Thus, the competition between the release and mobility of the surfactant molecules affects the OMEC behavior. In the start of mixing process, the surfactant release process is faster as compared to the immobilization process, resulting in an increase of conductance. After reaching a local maximum, the release process of surfactant slows down but the immobilization process still goes on. Hence, in this mixing period more surfactants are immobilized than released, and consequently, the OMEC decreases.

The SAXS profiles of HNBR/clay and ENR/clay nanocomposites, recorded at various mixing times are depicted in Figure 2(a,b), respectively. The position of peak represents the interlayer spacing of the organoclay in the nanocomposite. In Figure 2(a), as the mixing time increases, the peak position shifts to $q = 0.15$ Å^{-1} corresponding to interlayer spacing of 4.2 nm, which is attributed to the diffusion of more and more HNBR chain into the clay galleries. Further, it can be observed that the scattering intensity decreases with mixing time, an indication that the intercalated clay structure is destroyed. It could be due to exfoliation of clay tactoids in the polymer matrix. The position and height of the peak remain unchanged during the mixing time span from 4 to 30 min. This suggests that the final state of morphology that consists of intercalated and exfoliated structure of clay has reached after 4 min of mixing time. This also explains the plateau of the online measured electrical conductance after 4 min as is shown in Figure 1(a).

The SAXS profiles of ENR/clay nanocomposite after various mixing times are depicted in Figure 2(b). The decrease of peak height, in the period up to 4 min of mixing time, implies that the clay layers are exfoliated to some extent in the polymer matrix. However, it can be observed that the peak does not disappear completely and its position and shape do not change with further increase in mixing time up to the recorded 10 min. This suggests that the final morphology has reached in 4 min and that the final morphology could consist of intercalated and exfoliated clay structures. The interaction between ENR and

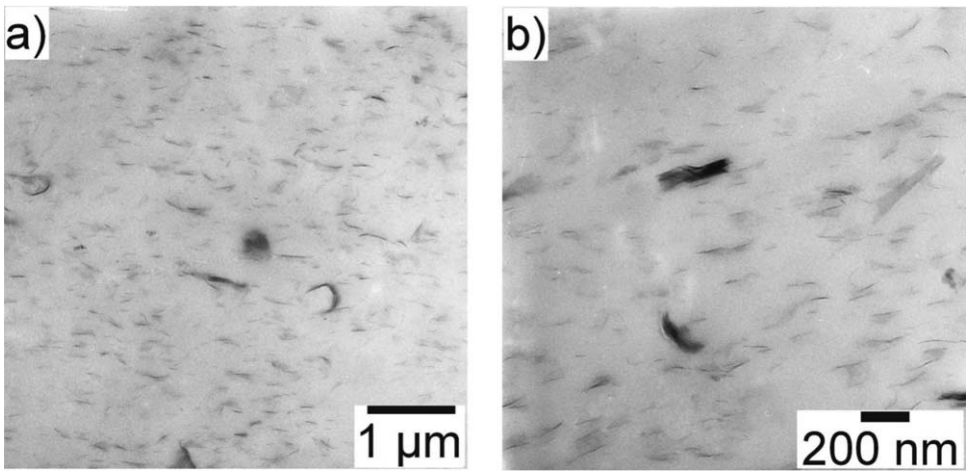

Figure 4. TEM micrographs: (a) low magnification, (b) high magnification of ENR/clay nanocomposite after 4 min of mixing time.

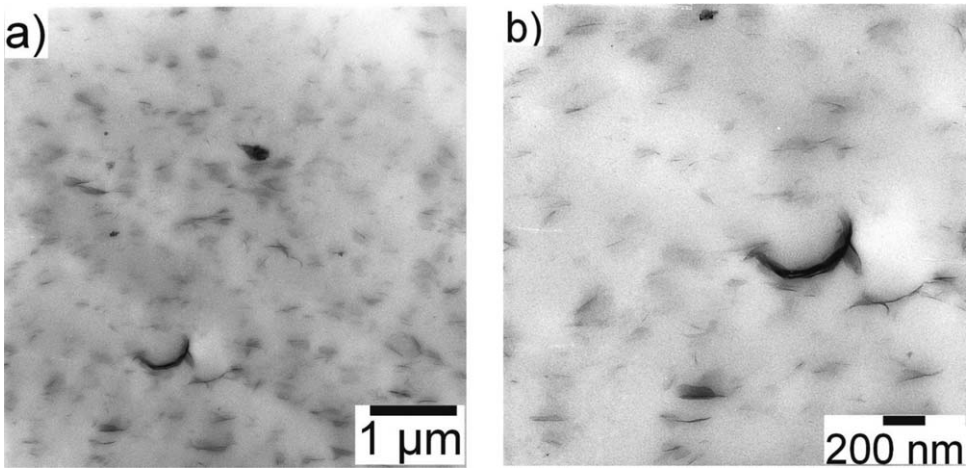

Figure 5. TEM images of ENR/clay nanocomposites after 10 min of mixing time: (a) low magnification and (b) high magnification.

surfactant molecules could facilitate the quick insertion of ENR chains into the clay galleries during compounding.[30] However, on the other hand the bulky group formed by the interaction of the surfactant and epoxy group of the rubber lowers the chain mobility and slows down the infiltration rate, and therefore, hampers the exfoliation process of the intercalated structures. Varghese *et al.*[31] prepared ENR/clay nanocomposites using different types of clays and they also obtained nanocomposites with both intercalated and exfoliated structures.

The microdispersion of clay in HNBR was visualized by AFM as presented in Figure 3. It can be seen that the big agglomerates are broken down into smaller aggregates in 4 min mixing [Figure 3(a,b)]. In Figure 3(b,c), it can also be observed that there are clay tactoids with 100 nm in size and the morphology remained unchanged with longer mixing time. This explains the OMEC plateau in this time span [Figure 1(a)]. But, longer mixing time, however, does improve the distribution of clay tactoids in the polymer matrix [Figure 3(c)].

Microdispersion of organoclay in ENR matrix has been characterized by TEM. Figure 4 shows the TEM images (at low and high magnification) of the ENR/clay nanocomposite after 4 min of mixing time. It can be seen that clay is uniformly dispersed along with few aggregates, representing a mixed morphology of intercalated and exfoliated clay structures. This reinforces the SAXS results discussed above. A similar mixed morphology was also reported by Varghese *et al.*[31]

Figure 5 shows the TEM micrographs of ENR/clay nanocomposite after mixing time of 10 min. This morphology is similar to that of nanocomposite after 4 min of mixing time (see Figure 4). This implies that beyond 4 min of mixing time, morphology of the nanocomposite does not change. The consumption of the released surfactant molecules due to interaction with epoxy group in the ENR chains causes a reduction of the OMEC values [Figure 1(b)].[30]

EFFECT OF ORGANOCLAY ON MORPHOLOGY DEVELOPMENT IN HNBR/ENR BLENDS

Online Conductance of Unfilled and Filled HNBR/(ENR/Clay) Blend

Online measured electrical conductance profiles of unfilled HNBR/ENR and filled HNBR/(ENR/clay masterbatch) blend as function of mixing time are shown in Figure 6. The OMEC signal of unfilled HNBR/ENR (50/50) blend (curve 1) is quite low,

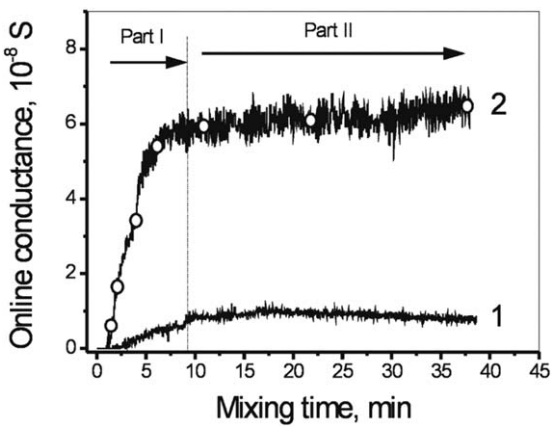

Figure 6. The OMEC profiles of the HNBR/ENR blend (curve 1) and HNBR/(ENR/clay masterbatch) blend (curve 2) versus mixing time.

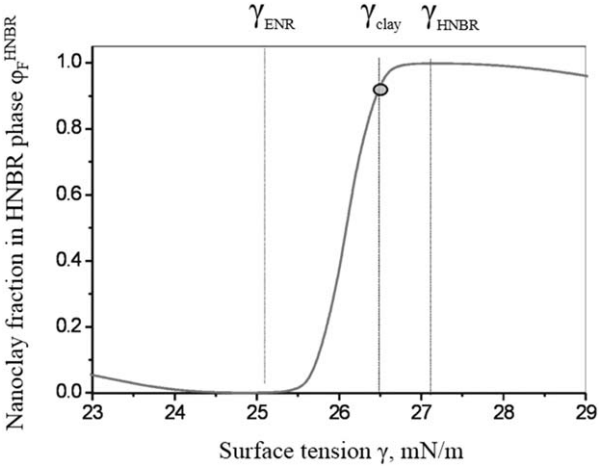

Figure 7. Master curve of filler distribution in a 50/50 HNBR/ENR blend calculated by means of the Z-model (with $n = 1$).

Table I. Surface Tensions Data of the Materials

Materials	Surface tension, mN/m
HNBR	27.2
ENR	25
Nanoclay	26.5

which is mainly originated from the HNBR phase, because the online conductance of ENR is very small compared to that of HNBR. When the masterbatch of ENR/clay was mixed with virgin HNBR, the online conductance increased and reached a plateau value after a short mixing time (curve 2). For clarity, the online measured electrical conductance background curve of HNBR/(ENR/clay masterbatch) is divided into two parts, i.e., part I and part II. It is supposed that the former part of the curve could be due to migration of organoclay from the relatively less polar ENR phase to the more polar HNBR phase. If the OMEC graph of HNBR/(ENR/nanoclay masterbatch) is compared with our previous investigations on HNBR/(NR/clay masterbatch) blend,[25] an important difference can be noted that the former shows plateau for longer mixing time, whereas for the later, the conductance starts decreasing after 15 min of mixing time. In order to explore the online conductance in Part II of the curve, the dispersion and distribution of organoclay as well as the dynamics of development of blend morphology was investigated with surface tension based model, SAXS, AFM, and TEM.

Investigation of Clay Transfer and Localization

Generally, the localization of filler in a polymer blend matrix depends on both the thermodynamics and kinetic factors.[32] On the basis of the Z-model proposed in our previous work, the clay localization in HNBR/ENR blend phases at an equilibrium state can be predicted using Eqs. (1−4).[33,34]

$$\frac{\varphi_F^{\mathrm{HNBR}}}{\varphi_F^{\mathrm{ENR}}} = n\left(\frac{\gamma_{\mathrm{ENR}}+\gamma_F-2\sqrt{\gamma_{\mathrm{ENR}}\gamma_F}}{\gamma_{\mathrm{HNBR}}+\gamma_F-2\sqrt{\gamma_{\mathrm{HNBR}}\gamma_F}}\right)^2 \quad (1)$$

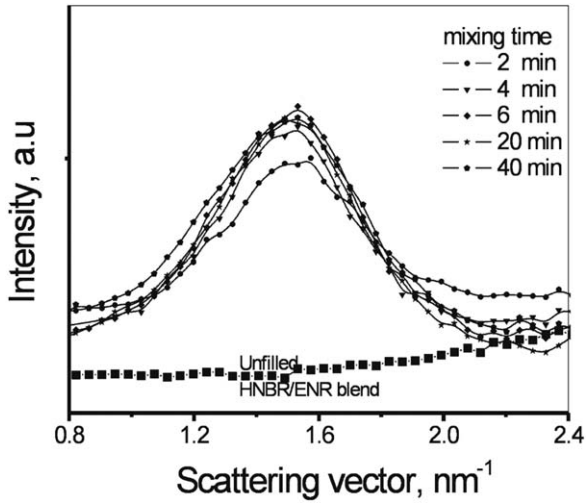

Figure 9. SAXS analysis of unfilled HNBR/ENR and filled HNBR/(ENR/clay masterbatch) blends at different mixing time.

$$\varphi_F^{HNBR}+\varphi_F^{ENR}=1 \quad (2)$$

$$\varphi_F^{HNBR}=\frac{n\omega}{n\omega+1} \quad (3)$$

with

$$\omega=\left(\frac{\gamma_{ENR}+\gamma_F-2\sqrt{\gamma_{ENR}\gamma_F}}{\gamma_{HNBR}+\gamma_F-2\sqrt{\gamma_{HNBR}\gamma_F}}\right)^2 \quad (4)$$

Where $\varphi_F^{\mathrm{HNBR}}$ and φ_F^{ENR} are the weight fractions of the filler F in the HNBR and ENR phase, respectively. γ_{HNBR}, γ_{ENR} and γ_F are the surface tensions of HNBR and ENR as well as filler F, respectively, and n is ratio HNBR to ENR in the blend.

Using the data of surface tension measurements given in Table I, the master curve of filler distribution in 50/50 HNBR/ENR blend was calculated and is presented in Figure 7. A clay fraction of

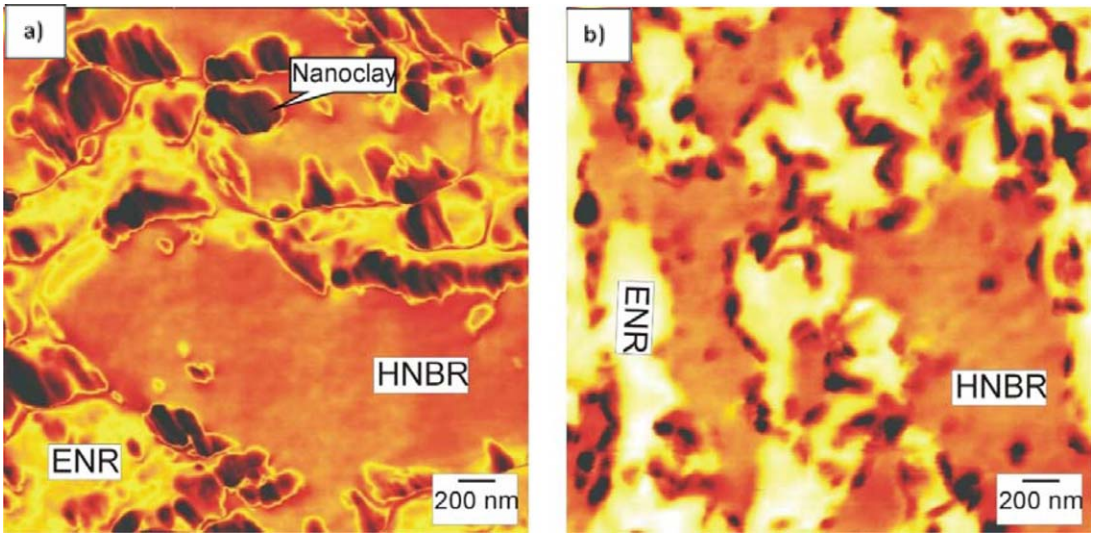

Figure 8. AFM micrographs of HNBR/(ENR/clay masterbatch) blends after: (a) 1.5 min (b) 40 min (light area: ENR, grey area: HNBR, black area: nanoclay). [Color figure can be viewed in the online issue, which is available at wileyonlinelibrary.com.]

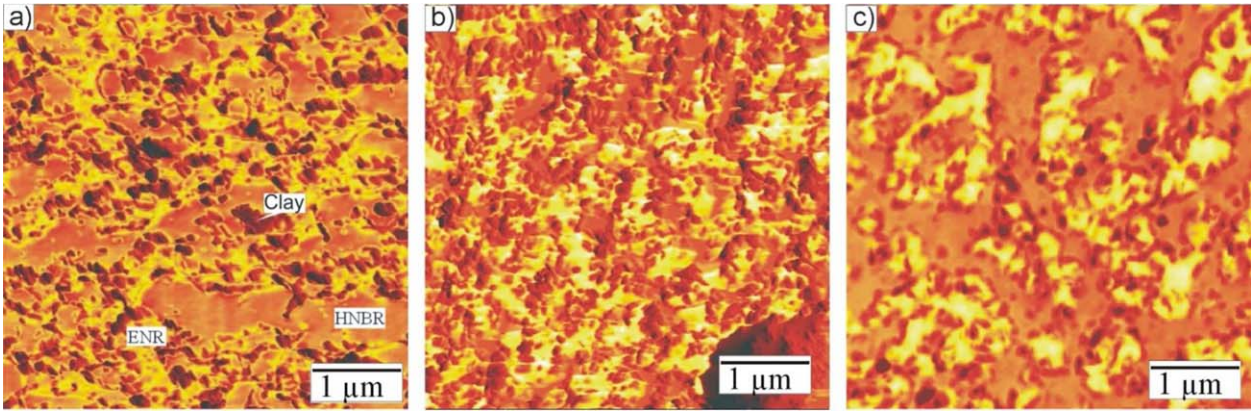

Figure 10. AFM micrographs: (a) 1.5, (b) 10, and (c) 40 min of HNBR/ENR/clay masterbatch) blends (light area: ENR, grey area: HNBR, black area: nanoclay). [Color figure can be viewed in the online issue, which is available at wileyonlinelibrary.com.]

about 0.9 localized in the HNBR phase, i.e., a complete localization of clay in the HNBR is predicted, when the filled HNBR/ENR blend reaches a thermodynamic equilibrium state.

In order to investigate the localization of clay experimentally, AFM micrographs of HNBR/(ENR/clay masterbatch) at the beginning of mixing process (after 1.5 min) and at the end of mixing process (40 min) were obtained and are depicted in Figure 8(a,b), respectively. The dark grey areas correspond to the HNBR phase and the light areas to the ENR phase, while the black areas represent the clay platelets/tactoids. At the beginning of mixing process all the clay platelets were present in the ENR phase [Figure 8(a)]. After 40 min of mixing time, majority of the clay platelets migrated to the darker phase, i.e., HNBR, as shown in Figure 8(b). The experimental determination of organoclay transfer from the ENR to HNBR phase is a confirmation of the prediction made by the surface tension model as discussed above. Furthermore, larger clay aggregates of ~100 nm size, well distributed in the ENR phase, can be seen in Figure 8(a), while after 40 min of mixing time, smaller organoclay particles (~50 nm), localized in the HNBR phase, were observed [Figure 8(b)]. The distribution of smaller organoclay particles in HNBR phase could be attributed to better dispersion of organoclay in HNBR than in ENR component. The clay aggregates are predominantly found in the HNBR areas closed to the interphase. The increase of the OMEC in the Part I (Figure 6) is, thus, due to the migration of clay from the ENR to the HNBR phase.

The SAXS profiles of HNBR/ENR and HNBR/(ENR/clay masterbatch) blends at different mixing times are shown in Figure 9. The SAXS patterns show that the peak position and height remain unchanged with increasing mixing time, suggesting that the intercalated structures nearly remain unchanged during the clay transfer from the ENR to the HNBR phase.

Development of Morphology in Nanoclay Modified HNBR/ENR Blends

The development of morphology in HNBR/(ENR/clay masterbatch) blend as a function of mixing time is followed by AFM as given in Figure 10. Analyzing the dynamics of morphological changes not only leads us to understand the Part II of OMEC curve (Figure 6) but also offers insight into the mechanism of clay transfer from ENR to HNBR phase as well as the phase inversion of blend morphology. After 1.5 min of mixing time, clay aggregates are observed in ENR matrix surrounding the unfilled HNBR domains. As the mixing time increases to 10 min, organoclay starts moving to the HNBR phase. At the same time, the morphology starts changing to a co-continuous morphology as depicted in Figure 10(b). Simultaneously, clay aggregates are broken into smaller sizes. During the mixing time

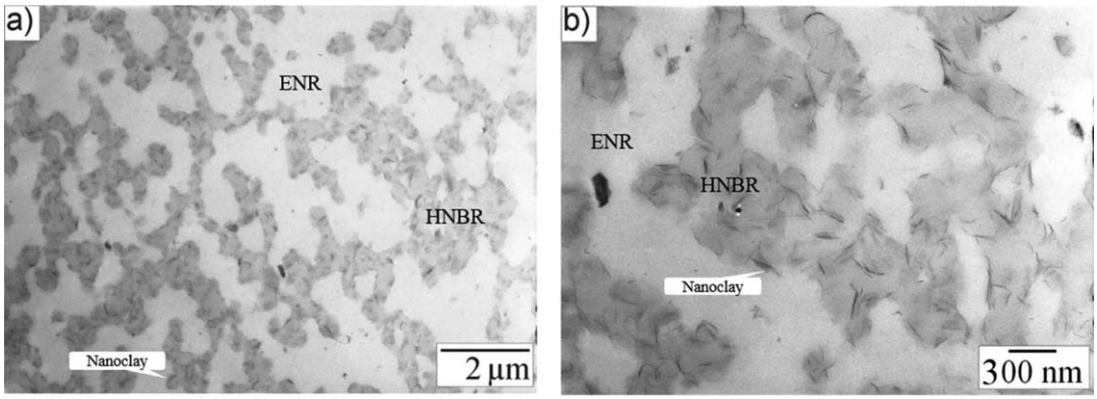

Figure 11. TEM micrographs: (a) low magnification (b) high magnification of HNBR/(ENR/clay masterbatch) blend after 40 min mixing time.

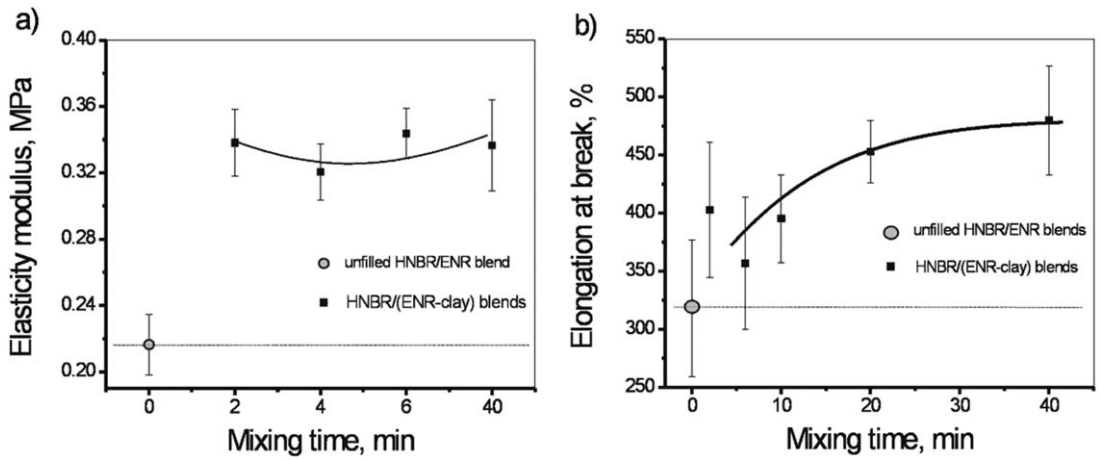

Figure 12. Tensile test results of HNBR/(ENR/clay masterbatch) as function of mixing time and corresponding unfilled blends: (a) tensile modulus, (b) elongation at break.

from 10 to 40 min, more clay platelets migrate from the ENR to HNBR phase as can be seen in Figure 10(c).

Figure 11(a,b) clearly show that after mixing time of 40 min, large number of the clay platelets have migrated to the HNBR phase. This also explains the plateau (Part II) of online conductance profile shown in Figure 6.

Investigation of Mechanical Behavior

The tensile properties of the virgin and HNBR/(ENR/clay) blends were also investigated. Figure 12(a) shows that the modulus of HNBR/(ENR/clay masterbatch) filled with 4.7 wt % organoclay is significantly higher than that of the virgin blend. Ray *et al.*[35] have also observed an increase in modulus of organoclay-filled blends and described it due to reinforcing efficiency and ability of the nanofiller to promote the interfacial adhesion between the immiscible phases. However, the mixing time seems not to influence the modulus, although, the morphology of the blend alters significantly as discussed above.

Figure 12(b) shows the elongation at break versus mixing time. The localization of nanoclay at the interface strengthens the phase adhesion and increases the resistance to failure. The increasing of strain at break with increasing mixing time could be due to better dispersion and distribution of organoclay in the HNBR phase and improved interfacial adhesion between the phases as has been reported by Ganter *et al.*[36] in the case of nanoclay filled SBR.

CONCLUSIONS

The online measured electrical conductance (OMEC) method has been employed to investigate the dynamics of migration and selective localization of nanoclay in hydrogenated acrylonitrile butadiene rubber (HNBR)/epoxidized natural rubber (ENR) blend systems. To understand OMEC profiles of the nanoclay/rubber composites, microscopic and X-ray scattering techniques were also used. It was observed that the online measured electrical conductance not only depends on the phase specific localization of organoclay but also on the blend morphology. The nanoclay was found to localize in the HNBR phase of the blend system as revealed by the OMEC data and atomic force and transmission electron microscopy. Further, the surface tension based model was also employed to study the dispersion of organoclay in the blend system, which also predicted the favorable localization of organoclay in HNBR phase, thus reinforcing the OMEC results. Finally, the mechanical behavior (tensile properties) of the organoclay/blend nanocomposite systems was evaluated as function of mixing time. The increasing of strain at break with the mixing time was observed which was attributed to better dispersion and distribution of organoclay in the HNBR phase and improved interfacial adhesion between the immiscible phases.

ACKNOWLEDGMENTS

The authors are grateful to Higher Education Commission (HEC) Pakistan and German Research Foundation (DFG) for the financial assistance. Special thanks to Dr. Z. Funke, Dr. K. Busse (InstitutfürChemie/PhysikalischeChemie der Polymere, Martin Luther University Halle-Wittenberg) for surface tension measurements and SAXS analysis, respectively and Dr. R. Godehardt (Institutfür-Physik, Martin Luther University Halle-Wittenberg, Germany) for transmission electron microscopic analysis.

REFERENCES

1. Usuki, A.; Kawasum, M.; Kojima, Y.; Fukushima, Y.; Okada, A.; Kurauchi, A.; Kamigaito, O. *J. Mater. Res* **1993**, *8*, 1174.
2. Ray, S. S.; Okamoto, M. *Prog. Polym. Sci.* **2003**, *28*, 1539.
3. Thostenson, E. T.; Li, C.; Chou, T. W. *Compos. Sci. Technol.* **2005**, *65*, 491.
4. Hussain, F.; Hojjati, M.; Okamoto, M.; Gorga, R. E. *J. Compos. Mater.* **2006**, *40*, 1511.
5. Paul, D. R.; Robeson, L. M. *Polymer* **2008**, *49*, 3187.
6. Herrmann, W.; Uhl, C.; Heinrich, G.; Jehnichen, D. *Polym. Bull.* **2006**, *57*, 395.

7. Ganter, M.; Gronski, W.; Reichert, P.; Mülhaupt, R. *Rubber Chem. Technol.* **2001**, *74*, 221.
8. Tsuruk, V. V. *Tribol. Lett.* **2001**, *10*, 132.
9. Wang, S.; Zhang, Y.; Peng, Z.; Zhang, Y. *J. Appl. Polym. Sci.* **2005**, *98*, 227.
10. Li, W.; Huang, D. Y.; Ahmadi, S. J. *J. Appl. Polym. Sci.* **2006**, *99*, 3275.
11. Karger-Kocsis, J.; Wu, C. M. *Polym. Eng. Sci.* **2004**, *44*, 1083.
12. Chow, W. S.; MohdIshak, Z. A.; Ishiaku, U. S.; Karger-Kocsis, J.; Apostolov, A. A. *J. Appl. Polym. Sci.* **2004**, *91*, 175.
13. Li, Y.; Shimizu, H. *Polymer* **2004**, *45*, 7381.
14. Khatua, B. B.; Lee, D. J.; Kim, H. Y.; Kim, J. K. *Macromolecules* **2004**, *37*, 2454.
15. Mehrabzadeh, M.; Kamal, M. R. *Can. J. Chem. Eng.* **2002**, *80*, 1083.
16. Fang, Z.; Harrats, C.; Moussaif, N.; Groeninck, G. *J. Appl. Polym. Sci.* **2007**, *106*, 3125.
17. Ray, S. S.; Pouliot, S.; Bousmina, M.; Utracki, L. A. *Polymer* **2004**, *45*, 8403.
18. Si, M.; Araki, T.; Ade, H.; Kilcoyne, A. L. D.; Fisher, R.; Sokolov, J. C.; Rafailovich, M. H. *Macromolecules* **2006**, *39*, 4793.
19. Wu, S. *Polym. Eng. Sci.* **1987**, *27*, 335.
20. Utracki, L. A. *J. Rheol.* **1991**, *35*, 1615.
21. Wang, Y.; Zhang, Q.; Fu, Q. *Macromol. Rapid Commun.* **2003**, *24*, 231.
22. Gelfer, M. Y.; Song, H. H.; Liu, L.; Hsiao, B. S.; Chu, B.; Rafailovich, M.; Si, M.; Zaitsev, V. *J. Polym. Sci. Part B: Polym. Phys.* **2003**, *41*, 44.
23. Hambir, S.; Bulakh, N.; Kodgire, P.; Kalgaonkar, R.; Jog, J. P. *J. Polym. Sci. Part B: Polym. Phys.* **2001**, *39*, 446.
24. Le, H. H.; Qamer, Z.; Ilisch, S.; Radusch, H. *J. Rubber Chem. Technol.* **2006**, *79*, 621.
25. Ali, Z.; Le, H. H.; Ilisch, S.; Busse, K.; Radusch, H.-J. *J. Appl. Polym. Sci.* **2009**, *113*, 667.
26. Epoxidized Natural Rubber. Weber & Schaer GmbH & Co, Available at: http://www.weber-schaer.com.
27. Fowkes, F. M. *J. Phys. Chem.* **1963**, *67*, 2538.
28. Ali, Z.; Le, H. H.; Ilisch, S.; Radusch, H.-J. *J. Mater. Sci.* **2009**, *44*, 6427.
29. Sadhu, S.; Bhowmick, A. K. *J. Polym. Sci. Part B: Polym. Phys.* **2004**, *42*, 1573.
30. Mohd Ishak, Z. A.; Wan, P. Y.; Wong, P. L.; Ahmad, Z.; Ishiaku, U. S.; Karger-Kocsis, J. *J. Appl. Polym. Sci.* **2002**, *84*, 2265.
31. Varghese, S.; Karger-Kocsis, J.; Gatos, K. G. *Polymer* **2003**, *44*, 3977.
32. Fenouillot, F.; Cassagnau, P.; Majeste, J.-C. *Polymer* **2009**, *50*, 1333.
33. Le, H. H.; Oßwald, K.; Ilisch, S.; Pham, T.; Stöckelhuber, K. W.; Heinrich, G.; Radusch, H. *J. Macromol. Mater. Eng.* **2011**, *297*, 464.
34. Le, H. H.; Osswald, K.; Ilisch, S.; Hoang, X. T.; Heinrich, G.; Radusch, H. -J. *J. Mater. Sci.* **2012**, *47*, 4270.
35. Ray, S. S.; Bousmina, M. *Macromol. Rapid Commun.* **2005**, *26*, 1639.
36. Ganter, M.; Gronski, W.; Semke, H.; Zilg, T.; Thomann, C.; Mülhlhaupt, R. *Kautsch. Gummi Kunstst.* **2001**, *54*, 166.